Direct Adaptive Input Shaping Using Supervisory Fuzzy System to Reduce Residual Vibration of an Uncertain Flexible-Link Robot

Withit Chatlatanagulchai[1,*], Chonlawit Prutthapong[2] and Naphon Thanapakorn[1]

[1]Control of Robot and Vibration (CRVLAB), Department of Mechanical Engineering, Faculty of Engineering, Kasetsart University, 50 Ngam Wong Wan Rd, Lat Yao, Chatuchak, Bangkok, 10900

[2]Julajomklao Navy Dockyard, The Royal Thai Naval Dockyard Headquarter, Moo 5, Laem Fa Pha, Samutprakarn, 10290

*Corresponding Author: fengwtc@ku.ac.th, Telephone Number 084-466-4472, Fax. Number 02-579-4576

Abstract

Input shaper's performance, in reducing the residual vibration from a point-to-point movement, degrades when system's natural frequencies and damping ratios change. We propose to adjust these parameters on-line using a supervisory fuzzy system. Experiments on a single flexible-link robot favor the adaptive over the un-adaptive cases.

Keywords: Adaptive Input Shaping, Vibration Reduction, Fuzzy System, Flexible-Link Robot.

1. Introduction

Input shaping is a method that devises an optimal FIR pre-filter. With optimized impulses' magnitude and timing, this pre-filter, when convoluted with the reference command, produces a shaped reference command that avoids exciting the system's vibrating modes, resulting in less residual vibration.

Since the method relies on the accurate knowledge of the system's natural frequencies and damping ratios, uncertainty from poor system identification or time-varying system can produce worse-than-optimal residual vibration.

To overcome this problem, more impulses have been added [1] – [3] and several adaptive input shaping schemes [4] – [6] have been proposed, each with pros and cons. More impulses lead to longer move time, and most adaptive schemes on-line estimate the system parameters, which falls short from the lack of persistent excitation of input and the divergence of parameter estimates.

In this paper, we present a novel idea where the impulses' magnitude and timing of the optimal pre-filter are changed on-line based on the amount of the residual vibration, which increases when the system is uncertain. Information on the residual vibration is fed to a fuzzy system, whose rule base is written such that the optimal pre-filter parameters are adjusted for less residual vibration, under the uncertainty.

This proposed technique was applied to a flexible-link robot with uncertain payload. The robot arm was commanded to move from point to point while its payload was regularly changed. An accelerometer at the tip measures the residual vibration. The experimental results show significant improvement on the residual vibration reduction over the un-adaptive case.

Section 2 presents the flexible-link robot system, the experimental setup, and finding the system's natural frequencies and damping ratios. Section 3 contains the design of the un-adaptive input shaper together with its experimental results. Section 4 explains the adaptive input shaper with its experimental results and discussions. Section 5 and 6 are conclusions and references.

2. Flexible-Link Robot System

2.1 Experimental Setup

Our flexible-link robot hardware, used in the experiments, is shown in Fig. 1. A one-foot steel ruler is used as the flexible link. Adjustable payload is placed at its tip. An accelerometer is attached at the tip, a strain gauge near the pivot, and an optical encoder to measure the DC motor's angle.

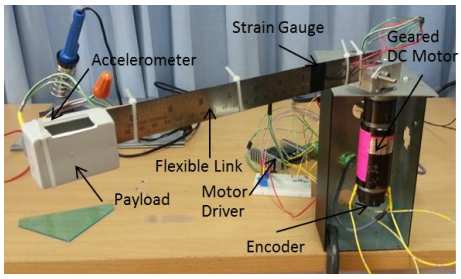

Fig. 1 The flexible-link robot hardware.

Its schematic diagram is given in Fig. 2, where θ is the motor angle, θ_s is additional angle of the payload as obtained from the strain gauge, $\theta_p = \theta + \theta_s$ is the payload angle, and a_p is the payload acceleration, measured from the accelerometer.

Fig. 3 shows our real-time control system setup. A National Instruments' system is used. Note that u is the control input sent to the motor driver.

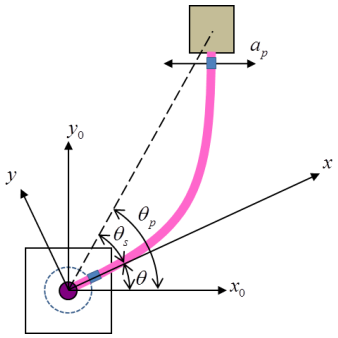

Fig. 2 Schematic diagram of the flexible-link robot.

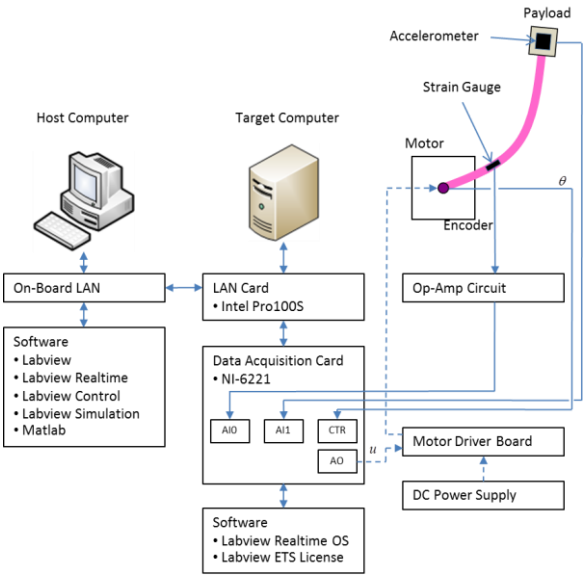

Fig. 3 Our real-time control system.

2.2 Finding Natural Frequencies and Damping Ratios

Because the input shaping needs the natural frequencies and damping ratios of the system, we performed a closed-loop experiment by having the reference motor angle θ_r be a sweep square wave with 20-degrees amplitude and sweeping frequencies from 0.1 to 0.5 Hz in 60 seconds. A PI controller with $k_p = 0.1$ and $k_i = 0.05$ was used. Fig. 4 contains the periodogram of a_p, showing the first-mode natural frequency of 13.2 Hz and the second-mode natural frequency of 24.5 Hz.

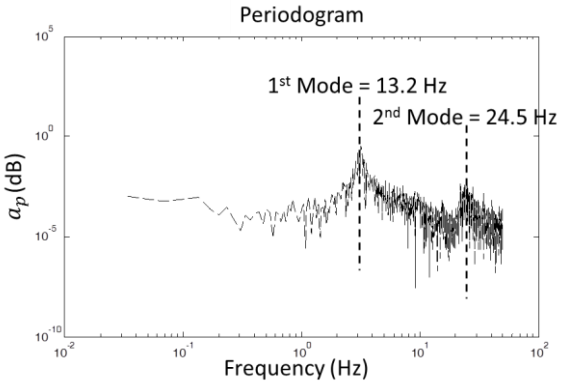

Fig. 4 Periodogram of a_p, showing the first and second modes.

We obtained the first-mode damping ratio by fixing one end of the flexible arm, giving initial angular displacement, then releasing and measuring θ_s with the strain gauge. Fig. 5 shows the result. From the logarithmic decrements formula, the damping ratio ζ was computed as

$$\delta = \frac{1}{n}\ln\frac{x_0}{x_n} = \frac{1}{5}\ln\frac{0.00532}{0.002891} = \frac{2\pi\zeta}{\sqrt{1-\zeta}},$$
$$\zeta = 0.0192.$$

We will use this damping ratio for both first mode and second mode.

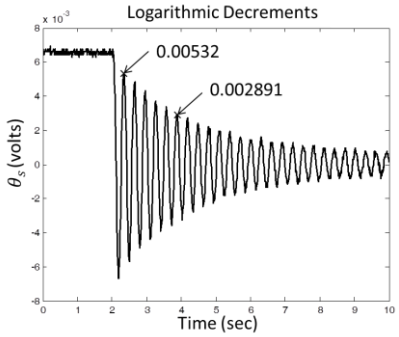

Fig. 5 Strain gauge signal to determine the damping ratio.

3. Un-adaptive Input Shaping

Fig. 6 contains a diagram of the un-adaptive input shaping, where F is the input shaper, C is the PI controller, P is the flexible arm, $\bar{\theta}_r$ is the motor reference angle, θ_r is the motor shaped reference angle, and e is the motor angle tracking error. Other variables were previously defined.

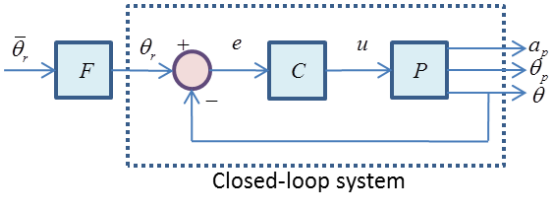

Fig. 6 Diagram of the un-adaptive input shaping.

The input shaper F uses the closed-loop natural frequencies and damping ratios as design parameters, which are un-changed in the un-adaptive case.

With the same PI controller as that of Section 2.2, and letting P be

$$P = \left(\frac{\bar{\omega}_{n1}^2}{s^2 + 2\bar{\zeta}_1\bar{\omega}_{n1}s + \bar{\omega}_{n1}^2}\right)\left(\frac{\bar{\omega}_{n2}^2}{s^2 + 2\bar{\zeta}_2\bar{\omega}_{n2}s + \bar{\omega}_{n2}^2}\right),$$ w

here $\bar{\omega}_{n1}, \bar{\omega}_{n2}, \bar{\zeta}_1,$ and $\bar{\zeta}_2$ are those of Section 2.2, the closed-loop natural frequencies and damping ratios of the first and second modes can then be computed as $\omega_{n1} = 21.105$ rad/sec, $\omega_{n2} = 153.804$ rad/sec, $\zeta_1 = 0.017,$ and $\zeta_2 = 0.019.$

The input shaper F can be written as an FIR filter

$$F(z) = F_1(z)F_2(z),$$

where

$$F_i(z) = \left(\bar{F}_1 + \bar{F}_2 z^{-\frac{t_2}{t_s}} + \bar{F}_3 z^{-\frac{t_3}{t_s}}\right)$$

belongs to the i[th] mode, with

$$\bar{F}_1 = 1/\left(1+2K+K^2\right),$$
$$\bar{F}_2 = 2K/\left(1+2K+K^2\right),$$
$$\bar{F}_3 = K^2/\left(1+2K+K^2\right),$$
$$K = e^{\frac{-\zeta\pi}{\sqrt{1-\zeta^2}}}, t_2 = \frac{\pi}{\omega_n\sqrt{1-\zeta^2}}, t_3 = \frac{2\pi}{\omega_n\sqrt{1-\zeta^2}},$$

t_s is the sampling time, and z is the z-transform operator. Details on the input shaper can be found in [7] and [8].

Since the input shaper was designed when there was no payload, we therefore expect performance deterioration when the payload exists. We use Thai five-baht coins as our payload.

In Fig. 7, we divide the experimental results into three parts: when input shaping is off and no payload, when input shaping is on and no payload, and when input shaping is on but with nine-coins payload.

Fig. 7(a) shows motor angle θ and its reference θ_r. We let $\bar{\theta}_r$ be a square wave with

twenty-degrees amplitude and twenty-seconds period. With the PID controller, θ follows θ_r quite well with more overshoot when input shaping is off. Note the tapering shape of the motor shaped reference angle θ_r as a result of convoluting with train of impulses.

In Fig. 7(b), the payload angle θ_p has long settling time when input shaping is off because the flexible link oscillates badly. When input shaping is turned on with no payload, the flexible link almost stops oscillating. However, when nine-coins payload is added, the flexible link starts to oscillate again because of changes in system's natural frequencies and damping ratios.

Fig. 7(c) shows the payload acceleration a_p which agrees with those results in Fig. 7(b).

The payload acceleration must be put in a quantifiable form for us to be able to reduce it. For that we design a quantity

$$\hat{a}_p = \int |a_p| dt,$$

where the integration is taken over the preceding movement of the flexible link. Fig. 7(d) shows this quantity. We see that without input shaping and no load $\hat{a}_p \approx 1$. When the input shaping is turned on, $\hat{a}_p \approx 0.13$. And later when the payload is nine coins, $\hat{a}_p \approx 0.3$. Therefore, we will set

$$\hat{a}_{pr} = 0.13$$

as our target value for $\hat{a}_p$.

Fig. 7(e) shows the control effort u. Note another benefit of the input shaping in reducing the peak control effort.

4. Adaptive Input Shaping

When payload changes, the performance degradation we found in the un-adaptive case is because the actual system's natural frequencies and damping ratios change with the payload but the un-adaptive input shaping was designed based on fixed natural frequencies and damping ratios. We propose a fuzzy supervisory system to adjust these design parameters on-line.

Fig. 8 depicts the diagram of the adaptive input shaping, where FS is the fuzzy supervisory system, $\hat{a}_{pt}$ is trend of $\hat{a}_p$ and is defined by

$$\hat{a}_{pt}(t) = \hat{a}_p(t) - \hat{a}_{p,ave}(t),$$

where $\hat{a}_{p,ave}(t)$ is average of $\hat{a}_p$ over a specified past time, ω_{n1t} is trend of ω_{n1} and is defined by

$$\omega_{n1t}(t) = \omega_{n1}(t) - \omega_{n1,ave}(t),$$

where $\omega_{n1,ave}(t)$ is average of ω_{n1} over a specified past time, d is an indicator whether the payload is increased or decreased, $\Delta\omega_{n1}$, $\Delta\omega_{n2}$, $\Delta\zeta_1$, and $\Delta\zeta_2$ are design parameter changes given to the adaptive input shaper. Other variables were previously defined.

The fuzzy supervisory system has three inputs and one output. The first input is $i_1 = \hat{a}_{pr} - \hat{a}_p$, which is negative if the oscillation of the flexible link is higher than our target. The second input is $i_2 = \hat{a}_{pt}$, which is negative if the oscillation is decreasing, and vice versa. The third input is $i_3 = \omega_{n1t}$, which is negative if the first-mode natural frequency used in the input shaper is decreasing, and vice versa. The output is $o = \Delta\omega_{n1}$, which will be added to ω_{n1} for the input shaper.

Readers who are not familiar to fuzzy control can consult [9] for some background. Linguistic rules were designed on the following human expert's decisions:

1) If the oscillation is higher than the target, we should adjust the design parameters of the input shaper, which are $\omega_{n1}, \omega_{n2}, \zeta_1$, and ζ_2. If not, no adjustment is needed.

2) Since we do not know the amount of payload changes, we must adjust the design parameters

for decreasing oscillation. Therefore, if oscillation decreases, continue adjusting the design parameters in the same direction as before. If oscillation increases, adjust the design parameters in the opposite direction.

3) A knowledge of whether the payload is increased or decreased helps initialize the design parameter adjustment in the right direction because increasing payload results in decreasing natural frequencies and damping ratios, and vice versa. This fact can be seen from a simple 1-DOF m-c-k system, of which we have

$$\omega_n = \sqrt{\frac{k}{m}}, \zeta = \frac{c}{2\sqrt{km}}. \quad (1)$$

Tables 1 – 3 are tabular representations of all 75 possible rules from the human expert's decisions above, which can be put in terms of input and output variables as follows:

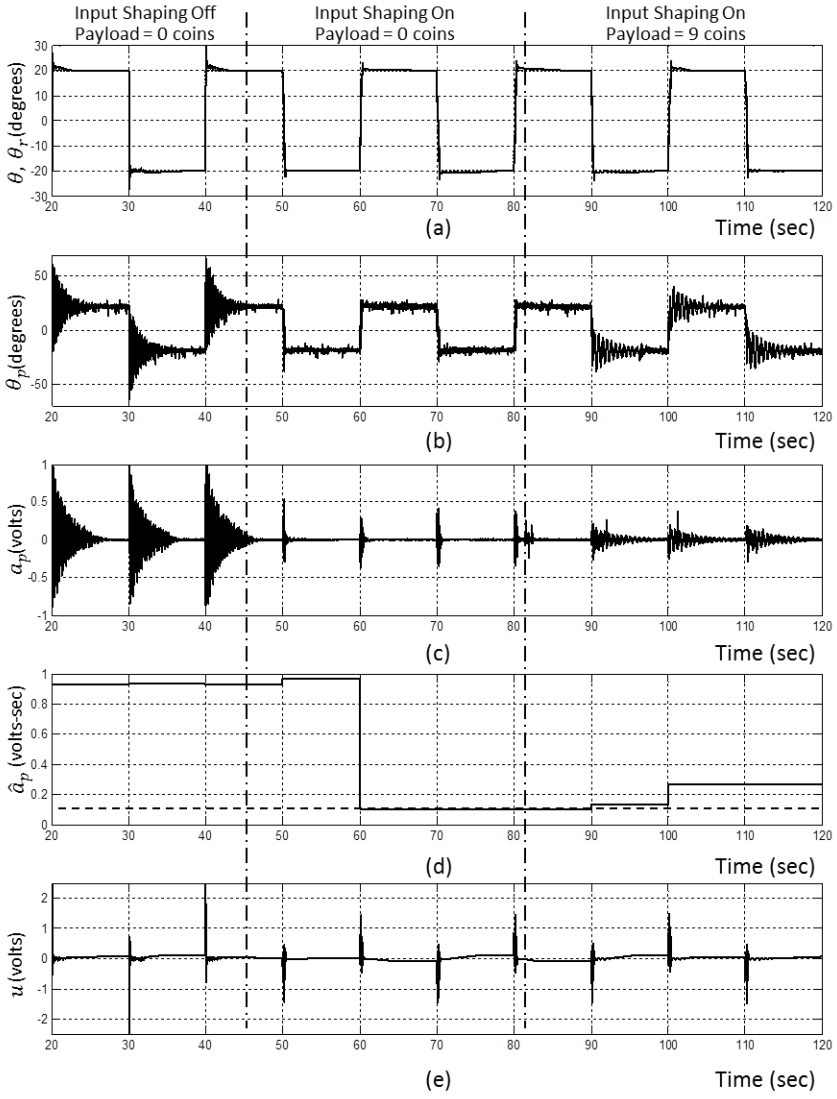

Fig. 7 Experimental results for un-adaptive input shaping. (a) Motor angle θ and its reference θ_r. (b) Payload angle θ_p. (c) Payload acceleration a_p. (d) Accumulated absolute acceleration $\hat{a}_p$. (e) Control effort u.

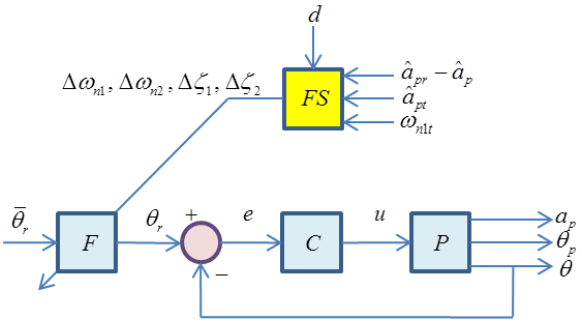

Fig. 8 The adaptive input shaping.

1) If i_1 is more negative, more o must be used. If i_1 is zero or positive, o should be zero.

2) If i_2 is negative, o should be such that i_3 is in the same direction as before. If i_2 is positive, o should be such that i_3 is in the opposite direction.

3) If $d=1$ (payload increases), -0.05 is added to o to emphasize decreasing direction. If $d=0$ (payload decreases), +0.05 is added to o to emphasize increasing direction.

Table. 1 Fuzzy rule-base when $i_1=-2$.

$i_1=\hat{a}_{pr}-\hat{a}_p=-2$					
$o=\Delta\omega_{n1}$	$i_2=\hat{a}_{pt}$				
$i_3=\omega_{n1t}$	-2	-1	0	1	2
-2	-2	-2	0	2	2
-1	-2	-2	0	2	2
0	0	0	0	0	0
1	2	2	0	-2	-2
2	2	2	0	-2	-2

Table. 2 Fuzzy rule-base when $i_1=-1$.

$i_1=\hat{a}_{pr}-\hat{a}_p=-1$					
$o=\Delta\omega_{n1}$	$i_2=\hat{a}_{pt}$				
$i_3=\omega_{n1t}$	-2	-1	0	1	2
-2	-1	-1	0	1	1
-1	-1	-1	0	1	1
0	0	0	0	0	0
1	1	1	0	-1	-1
2	1	1	0	-1	-1

Table. 3 Fuzzy rule-base when $i_1=0$.

$i_1=\hat{a}_{pr}-\hat{a}_p=0$					
$o=\Delta\omega_{n1}$	$i_2=\hat{a}_{pt}$				
$i_3=\omega_{n1t}$	-2	-1	0	1	2
-2	0	0	0	0	0
-1	0	0	0	0	0
0	0	0	0	0	0
1	0	0	0	0	0
2	0	0	0	0	0

All membership functions are given in Fig. 9. Note that they are normalized to -1 to 1, so there must be input and output gains.

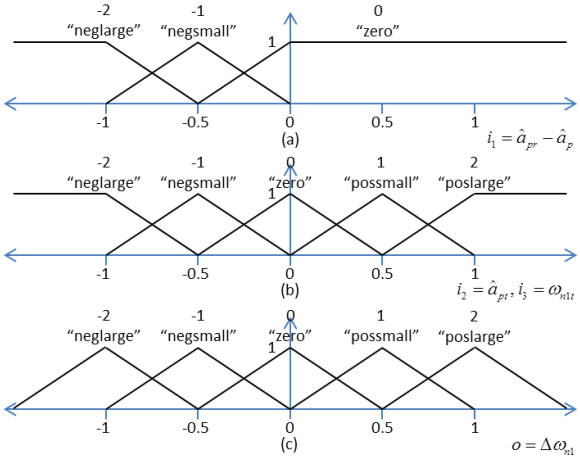

Fig. 9 Membership functions for the fuzzy supervisory system.

Note that we only have one output $o=\Delta\omega_{n1}$. Remaining design parameter changes, which are $\Delta\omega_{n2}$, $\Delta\zeta_1$, and $\Delta\zeta_2$ can be computed from Eq. (1) under some assumptions. With $\bar{\omega}_{n1}$ and $\bar{\zeta}_1$ known, and mass m can be measured quite accurately, we can compute c and k of the flexible link from Eq. (1). Assuming c and k are constant while m changes, then $\Delta\omega_{n1}/\Delta\zeta_1$ and hence $\Delta\zeta_1$ can be found from Eq. (1). With further assumptions that

$$\frac{\Delta\omega_{n1}}{\omega_{n1}}=\frac{\Delta\omega_{n2}}{\omega_{n2}}, \frac{\Delta\omega_{n1}}{\Delta\zeta_1}=\frac{\Delta\omega_{n2}}{\Delta\zeta_2},$$

$\Delta\omega_{n2}$ and $\Delta\zeta_2$ can then be found.

In our experiments, we used "minimum" inference mechanism, "center of gravity" defuzzification, input gains of $g_1=3$, $g_2=7$, and $g_3=1$, output gain of $h=0.01$. $\hat{a}_{p,ave}(t)$ and $\omega_{n1,ave}(t)$ are averaged over 1,000 past time steps. The sampling time t_s is 0.01 sec. The adaptive input shaping algorithm in Fig. 8 was

implemented on-line using Labview Control Design and Simulation Module.

Fig. 10 contains our experimental results. We divide the experiment into five parts, each with different payload. The input shaper and fuzzy supervisor are turned on at all time. In the first part, when the payload changes from 0 to 9 coins, the fuzzy supervisor adjusts ω_{n1}, used by the input shaper, from 21.105 to 13.01 rad/sec. The oscillation gradually falls under our target as seen from $\hat{a}_p$. In the second part, when the payload changes from 9 to 0 coins, the flexible link experiences a large oscillation with $\hat{a}_p = 0.66$ volts-sec before falling under our target as the fuzzy supervisor adjusts ω_{n1} from 13.01 to 22.56 rad/sec. In the third and fourth parts, when the payload changes from 0 to 6 coins and 6 to 3 coins respectively, the fuzzy supervisor is able to adjust ω_{n1} to appropriate levels of 15.53 and 19.73 rad/sec, resulting in less oscillation within the target. In all the parts above, the payload is changed abruptly. In the fifth part, we now gradually increase the payload from 3 to 4 to 5 to 6 coins. The fuzzy supervisor also adjusts ω_{n1} gradually from 19.73 to 18.22 to 17.53 to 15.53 rad/sec.

Fig. 10(c) to (f) shows corresponding fuzzy inputs and output. The output is confined to ± 1 range, and mostly the inputs are in ± 1 range, except around 200 seconds when the oscillation increases sharply.

5. Conclusions

Traditional input shaper is designed from fixed natural frequencies and damping ratios of the system. When system changes, these design parameter changes, and input shaper's performance degrades. We propose a way to continuously adjust the parameters on-line according to the residual vibration amount using fuzzy logic. A fuzzy supervisory system incorporates a way human adjusts the design parameters, when system changes, to bring the residual vibration down to a target. Our proposed adaptive system has shown to be effective in bringing the residual vibration down to the target when the payload changes both abruptly and gradually, increasing and decreasing.

Future work includes comparing the proposed adaptive input shaping to robust input shapers such as ZVD or ZVDD in terms of residual vibration and settling time.

6. References

[1] Sung, Y.-G. and Singhose, W.E. (2009). Robustness analysis of input shaping commands for two-mode flexible systems, *IET Control Theory and Applications*, vol.3(6), pp. 722 – 730.

[2] Vaughan, J., Yano, A. and Singhose, W. (2008). Comparison of robust input shapers, *Journal of Sound and Vibration*, vol.315, pp. 797 – 815.

[3] La-orpacharapan, C. and Pao, L.Y. (2005). Fast and robust control of systems with multiple flexible modes, *IEEE/ASME Transactions on Mechatronics*, vol.10(5), October 2005, pp. 521 – 534.

[4] Pereira, E., Trapero, J.R., Diaz, I.M. and Feliu, V. (2012). Adaptive input shaping for single-link flexible manipulators using an algebraic identification, *Control Engineering Practice*, vol.20, pp. 138 – 147.

[5] Cutforth, C.F. and Pao, L.Y. (2004). Adaptive input shaping for maneuvering flexible structures, *Automatica*, vol.40, pp. 685 – 693.

[6] Tzes, A. and Yurkovich, S. (1993). An adaptive input shaping control scheme for vibration supression in slewing flexible structures, *IEEE Transactions on Control Systems Technology*, vol.1(2), June 1993, pp. 114 – 121.

[7] Chatlatanagulchai, W. and Saeheng, K. (2009). Real-time reference position shaping to reduce vibration in slewing of a very flexible-joint robot, *Journal of Research in Engineering and Technology*, vol.6(1), January 2009, pp. 51 – 66.

[8] Chatlatanagulchai, W. and Prutthapong, C. (2009). Input shaping to reduce vibration in human-operated very –flexible-link robot manipulator, *KKU Engineering Journal*, vol.36(1), January 2009.

[9] Passino, K.M. and Yurkovich, S. (1997). Fuzzy Control, Addison Wesley.

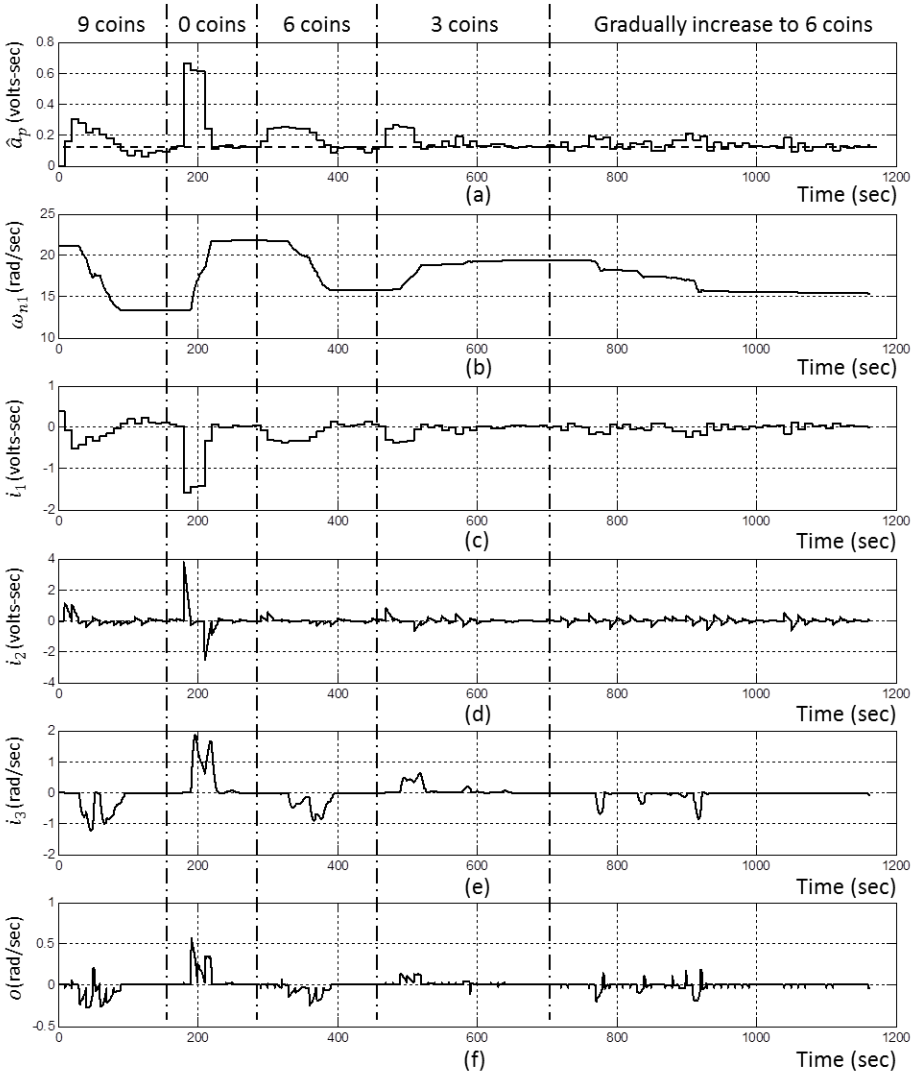

Fig. 10 Experimental results for adaptive input shaping. (a) Accumulated absolute acceleration $\hat{a}_p$. (b) First-mode natural frequency ω_{n1}. (c) First input to the fuzzy system: $\hat{a}_{pr} - \hat{a}_p$. (d) Second input to the fuzzy system: $\hat{a}_{pt}$. (e) Third input to the fuzzy system: ω_{n1t}. (f) Output from the fuzzy system: $\Delta\omega_{n1}$.